

# CONTROL/STRUCTURE INTERACTION DURING SPACE STATION FREEDOM-ORBITER BERTHING

T. Hua and E. Kubiak

NASA Johnson Space Center, Mail Code EG2

Houston, Texas 77058

Yeongching Lin, M. Kilby and J. Mapar

Dynacs Engineering Co., Inc.

1110 NASA Road 1, Suite 650

Houston, Texas 77058

## INTRODUCTION

The berthing maneuver is essential for the construction and assembly of Space Station Freedom (SSF) and has a direct effect on the SSF assembly build up and SSF/Orbiter operations. The effects of flexible body dynamics coupled with the available control system may impose new requirements on the maneuver. The problem is further complicated by the effect of the SSF control system on the Shuttle Remote Manipulator System (SRMS) (Figure A-1). These effects will play a major role in the development of operational requirements which need to be identified and validated in order to assure total safety and maneuver execution during SSF construction. This paper presents the results of ongoing studies to investigate the Control/Structure Interaction (CSI) during the berthing operations. The problem is formulated in terms of multi-flex body equations of motion for SSF and the SRMS and on-orbit flight control systems for the SRMS and the SSF, which includes the Control Moment Gyro (CMG) and Reaction Control System (RCS) Attitude Control Systems (ACS). The SSF control system designs are based on the Preliminary Design Review (PDR) version of the Honeywell design (Reference 1). The simulation tool used for the analysis is briefly described and the CSI results are presented for given berthing scenarios.

This paper also presents preliminary results of the verification of a new software analysis tool. This tool, referred to as the Station/Orbiter Multi-flex-body Berthing Analysis Tool (SOMBAT), is designed to analyze berthing operations for the Space Station Manned Base

(SSMB). Specifically, the results presented in this paper focus on the dynamic interaction of the Orbiter and the Shuttle Remote Manipulator System (SRMS) (Reference 2) with the control systems of the SSMB during the berthing process.

For this paper, operations consist of the berthing of the completed Stage-5 Space Station to the Orbiter at the beginning of the flight MB-6. The SRMS is used to perform the berthing operation. The SSMB assumes control of the combined system of the space station, Orbiter, and SRMS for this flight. The berthing operation is of interest because of the large change in mass properties of the combined system and the dynamic interaction with the station Attitude Control System.

### ACRONYMS

<b>ACS</b>	- Attitude Control System
<b>CDR</b>	- Critical Design Review
<b>CMG</b>	- Control Moment Gyro
<b>DRM</b>	- Design Reference Mission
<b>DRS</b>	- Draper RMS Simulation
<b>GG</b>	- Gravity Gradient
<b>LVLH</b>	- Local Vertical, Local Horizontal
<b>MB-6</b>	- Mission Build 6
<b>MM</b>	- Momentum Management
<b>PDR</b>	- Preliminary Design Review
<b>RCS</b>	- Reaction Control System
<b>SES</b>	- System Engineering Simulator
<b>SOMBAT</b>	- Station/Orbiter Multi-body Berthing Analysis Tool
<b>SRMS</b>	- Shuttle Remote Manipulator System
<b>SSEIC</b>	- Space Station Engineering Integration Contractor
<b>SSF</b>	- Space Station Freedom
<b>SSMB</b>	- Space Station Manned Base
<b>TEA</b>	- Torque Equilibrium Attitude

### CRITICAL ISSUES

The following issues are of concern during the berthing operations :

- Limitations on SRMS
  - a. Flexibility of arms -  
The Space Station active attitude control may induce excessive loads on the SRMS flexure during berthing.
  - b. Payload capability -  
The SRMS has been certified to handle payloads below 65,000 pounds. However, berthing the Orbiter to the Station assembly stages will involve payloads varying from 37,000 to over 250,000 pounds.
  - c. Joint velocity limit -  
SRMS joint speeds are also affected by the weight of the payloads. The larger the payload, the slower the arms have to move.
- ACS attitude control authority
  - a. CMG and RCS -  
CMG's capability to hold the desired attitude of the combined vehicles and RCS fuel consumption during the whole berthing operation needs to be investigated.
  - b. Jet firing constraints -  
Jet pulsing frequency limit has to be imposed on RCS to avoid exciting the Station structures.
  - c. Mass property update -  
The knowledge of Orbiter/SRMS position and orientation is required to update mass properties and controller gains.
- Power and thermal constraints -  
Lack of power generation from the locked solar arrays may cause excessive discharge of the batteries. Without proper attitude control, the ammonia in the large articulating thermal radiator may freeze within 30 minutes.

### **SIMULATION TOOL - SOMBAT**

The Space Station is envisioned as a complex, multi-flexible body configuration in an open-tree topology. The equations of motion for such systems are non-linear and become very complicated. The solution approach must be developed carefully to provide the required fidelity and accuracy and at the same time minimize computational cost associated with the time history simulation. Analysis for simulating the control and multi-flexible structure interaction

was performed using the SOMBAT software package because the traditional finite element method is not capable to analyze large translational and rotational motion. This tool is used for the studies of various berthing scenarios between the SSMB and the Orbiter.

### Theoretical Developments

Because it is very difficult to derive a closed form solution for a given structure, finite element analysis is used to obtain the stiffness and mass matrices of the structure. Let  $\mathbf{q}$  be the total vector of independent coordinates or the degrees of freedom of the structure that includes three translational and three rotational rigid body motions. The motion of the flexible structure is governed by a set of second-order differential equations of motion that can be written in the following compact matrix form (References 3, 4):

$$\mathbf{M}\ddot{\mathbf{q}} + \mathbf{K}\mathbf{q} = \mathbf{u} + \mathbf{v} + \mathbf{w} \quad (1)$$

where  $\mathbf{M}$  is assumed to be a positive definite mass matrix associated with the independent coordinates which can be represented as

$$\mathbf{M} = \begin{bmatrix} \mathbf{m}_{rr} & \mathbf{m}_{r\theta} & \mathbf{m}_{rf} \\ \mathbf{m}_{\theta r} & \mathbf{m}_{\theta\theta} & \mathbf{m}_{\theta f} \\ \mathbf{m}_{fr} & \mathbf{m}_{f\theta} & \mathbf{m}_{ff} \end{bmatrix}$$

where

- $\mathbf{m}_{rr}$  - the rigid mass matrix
- $\mathbf{m}_{\theta\theta}$  - the rigid body inertia matrix
- $\mathbf{m}_{r\theta}$  - the mass center
- $\mathbf{m}_{rf}$  - the linear momentum
- $\mathbf{m}_{\theta f}$  - the angular momentum
- $\mathbf{m}_{ff}$  - the modal mass matrix

and  $\mathbf{K}$  is the system stiffness matrix. Both  $\mathbf{M}$  and  $\mathbf{K}$  may be time varying. The input  $\mathbf{u}$  is the vector of generalized external forces associated with the independent coordinates,  $\mathbf{v}$  is the quadratic velocity vector that includes the gyroscopic and Coriolis force components, and  $\mathbf{w}$  is the closed loop control vector. The derivation is based on a nodal body formulation and

provides a convenient approach to use finite element output data. The derivation of equations of motion is discussed in detail in References 3 and 4.

The flexible body modelling techniques in SOMBAT are:

- A system made up of multiple components where relative motion of the components is modelled through joint kinematics and dynamics
- Components are modelled separately via NASTRAN
- An "order-N" algorithm is used to solve the equations of motion
- Integration of station control system with multi-body dynamics

### **SOMBAT Functional Overview**

SOMBAT consists of several modules used in modelling the system under study, optimizing the software for the specific problem, simulating the problem and viewing the time history of the simulation. The organization of these modules is illustrated in Figure 1. These modules are:

- Model Definition (Setup) Module
- Symbolic Code Generator
- User Defined Code
- Simulation Shell
- Post Processing
- Optional Capabilities
- Flexible Body Data Preprocessor
- Inverse Kinematics Preprocessor (Appendix A)

### **SOMBAT Features**

SOMBAT incorporates numerous features that make it ideal for rapid studies of berthing scenarios. Features currently provided by SOMBAT include:

- A complete orbital environment
- Automated, symbolic code generation for efficient, problem-specific simulation
- Rigid and flexible nonlinear multi-body dynamics (open and closed chain)
- A kinematic model of the SRMS
- A dynamics model of the SRMS (rigid and flexible)
- Honeywell PDR and CDR versions of the station ACS

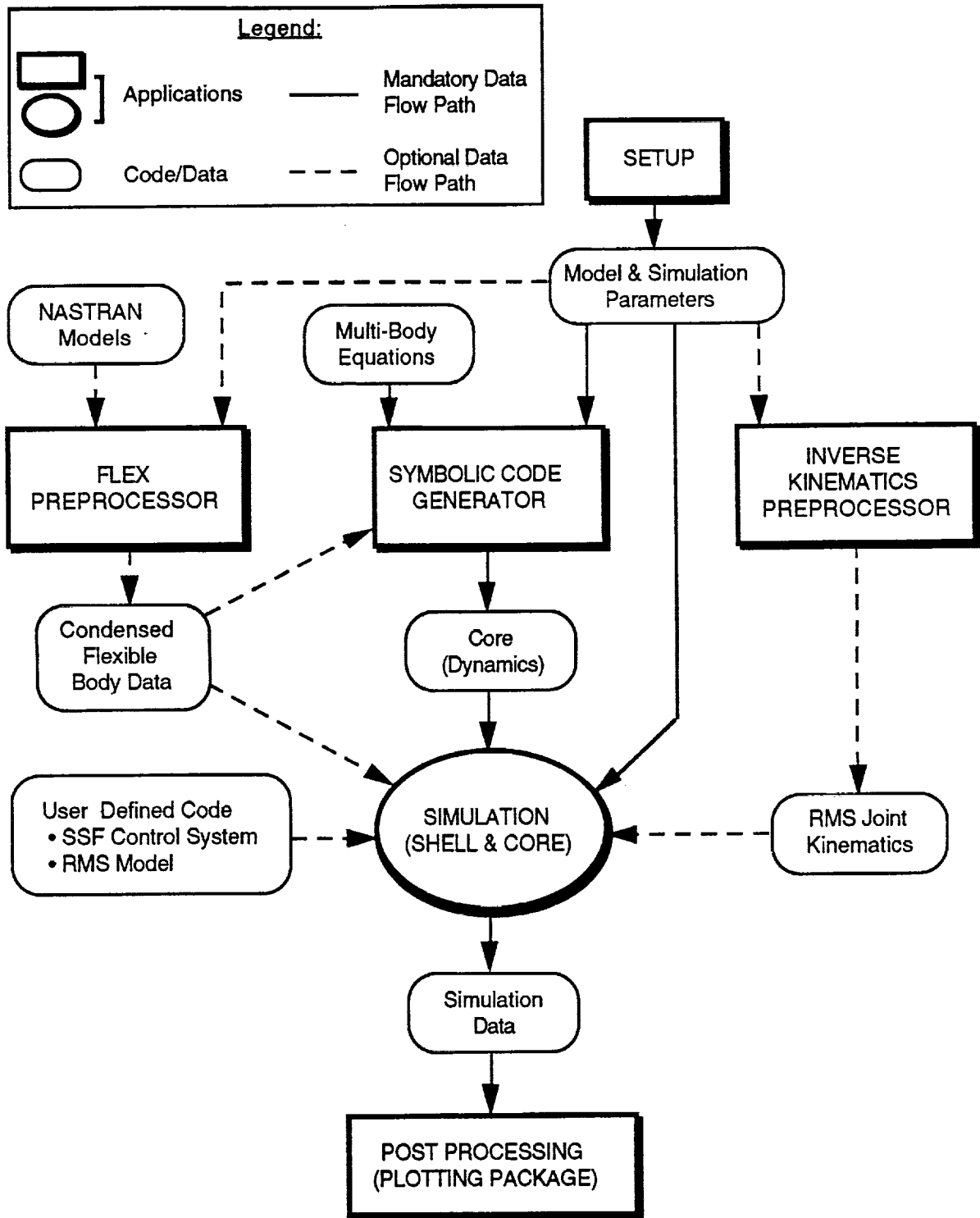


Figure 1: Organization of the SOMBAT Simulation Environment

- A high fidelity SRMS joint controller

## ANALYSIS RESULTS

This section evaluates the SSMB PDR control systems during the berthing of the complete Stage-5 Space Station to the Orbiter, Figure 2. The scenarios examined for the berthing operations are modelled after the timeline (Appendix B) in the Design Reference Mission (DRM) (Reference 5). This study focuses only on the SSMB control system and no evaluations of the Orbiter and SRMS control systems were performed. Motion between the Orbiter and SSMB is via the prescribed motion of the SRMS joints.

The system under study consisted of the Orbiter, the SRMS, and the SSMB. The mass properties for flight MB-5 were obtained from SSEIC's Model Management System (Reference 6). These models are

- Orbiter - a single rigid body
- SRMS - seven rigid links
- SSMB - five rigid (scenarios 1 and 2) or flexible bodies (scenario 3)

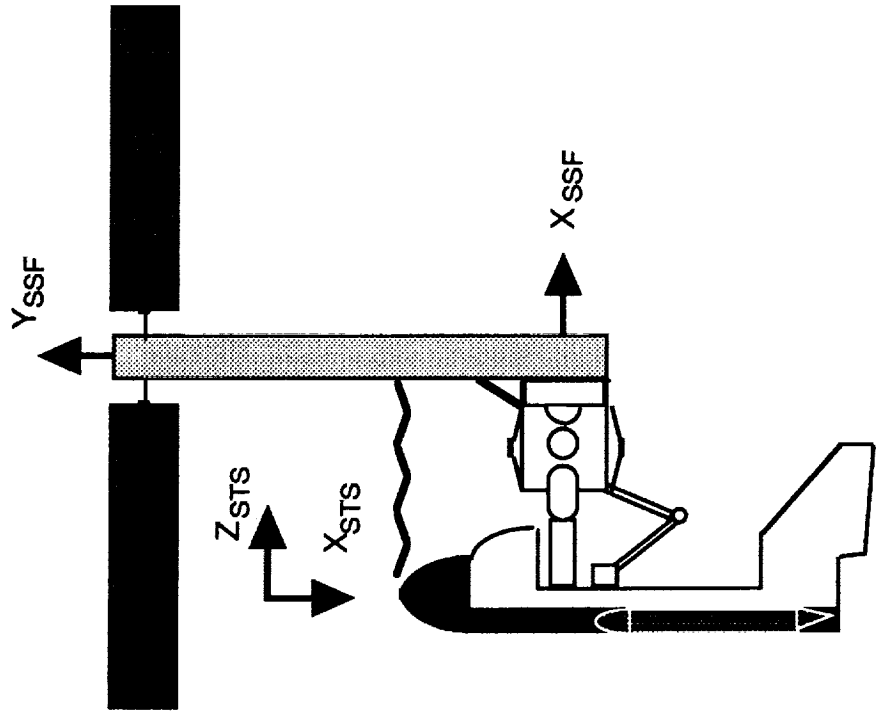
### Scenario 1

The scenario for case 1, illustrated in Figure B-1, considers the effects on the CMG/MM control system in maneuvering the combined structure to the TEA for the capture configuration from a gravity gradient attitude. The CMG retains control authority as the SRMS berths the SSMB to the Orbiter and then maintains the TEA for the berthed configuration. As shown by Figure 3, the scenario provides 10000 seconds for the CMG/MM system to maneuver to the capture TEA. After this period, the SRMS retracts the SSMB into the Orbiter payload bay for 3600 seconds followed by a period of 25000 seconds to achieve the berthed TEA.

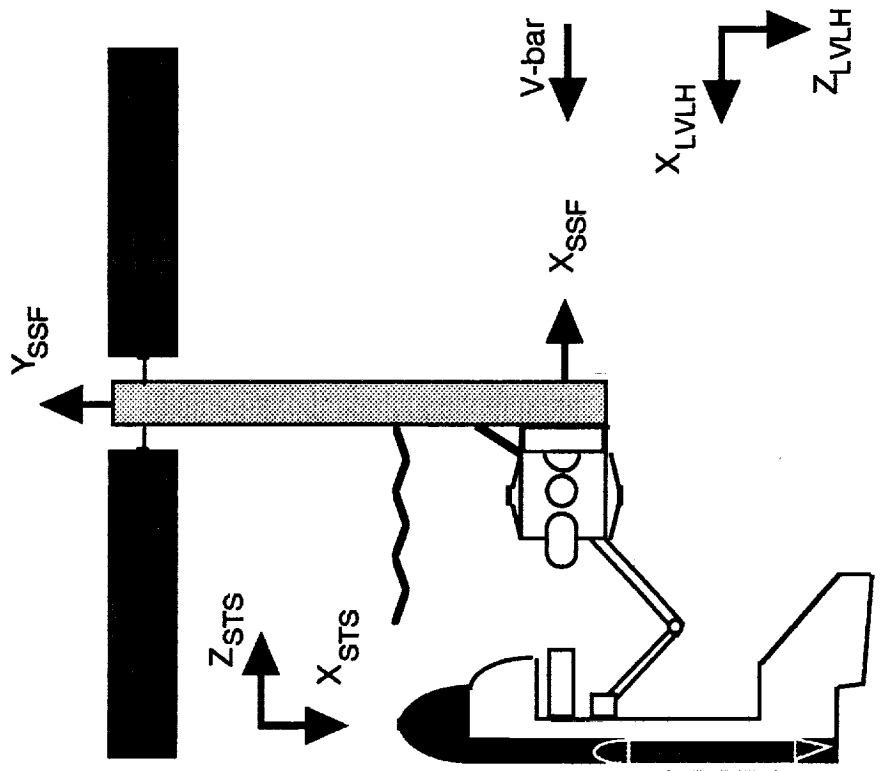
Figure 3-a shows the composite vehicle attitude. From this figure, two sets of transients are observed. The first transient response is produced by the maneuver to the capture TEA. The second set is associated with the SRMS motion. The difference in the capture TEA and the berthed TEA can also be observed by comparing the attitude at 12000 seconds (capture) and at 30000 seconds (berthed). This change in TEA results from the change in mass properties.

Figure 3-b illustrates the CMG momentum. These figures show the CMG momentum capacity of 14000 ft-lb-seconds to be exceeded by the maneuver from gravity gradient to TEA

**B: BERTHED**



**A: CAPTURE**



**Figure 2: Initial and Final Configurations of the Orbiter/SRMS/SSMB Stack for Berthing Operations**



and the SRMS retraction. As demonstrated by these results, the CMG/MM control system alone is unsuitable for the entire berthing operation.

### **Scenario 2**

Based on the previous results, another scenario, Figure B-2, is developed to examine the operation of the RCS and CMG control systems for the entire berthing operation. The RCS control system is used to move the composite system near the estimated capture TEA in 2000 seconds. This is followed by a handover to the CMG/MM system to achieve TEA. At 12000 seconds, SRMS retraction proceeds until the SSMB is mated to the Orbiter 3600 seconds later. After berthing, the CMG/MM seeks the new TEA for the berthed configuration.

Figure 4-a illustrates the combined system attitude. From this figure, the capture TEA is achieved at 12000 seconds and the berthed TEA at 25000 seconds. Figure 4-b shows the CMG momentum. As in the previous case, two transients occur for the RCS/CMG handover and for SRMS operations. Figure 4-b indicates the CMG momentum is not exceeded at the RCS/CMG handover, but is exceeded for the SRMS operations. Saturation is produced by the variation in mass properties during retraction by the the SRMS without a corresponding update in the feedback gains.

### **Scenario 3**

For this case, Figure B-3, a multi-flexible body station is examined. Usually, positioning a flexible structure, such as a space telescope or space station, will generally excite unwanted flexible modes in the structure. This case studies the oscillation in the elastic modes due to the jet firing. The scenario begins with the system in the capture configuration and is then commanded to the estimated TEA by the RCS control system. The estimated TEA for the capture configuration is 1.057 degrees (Roll), -22.889 degrees (pitch) and 14.137 (Yaw) with respect to LVLH.

Figure 5-a shows the attitude of the combined system. The commanded attitude is achieved after 1500 seconds. In Figure 5-b, the phase plane for the RCS indicates that the combined system is stable and controllable. Figure 5-c illustrates modal displacements of the first three modes of the core body. The natural frequencies of these modes are 0.483 Hz, 0.717 Hz, and 1.268 Hz. Figure 5-c indicates that the rigid body motion dominates the flexible body

**Units:**

TIME - seconds

THETA - degrees

Note: Euler 1-2-3 sequence

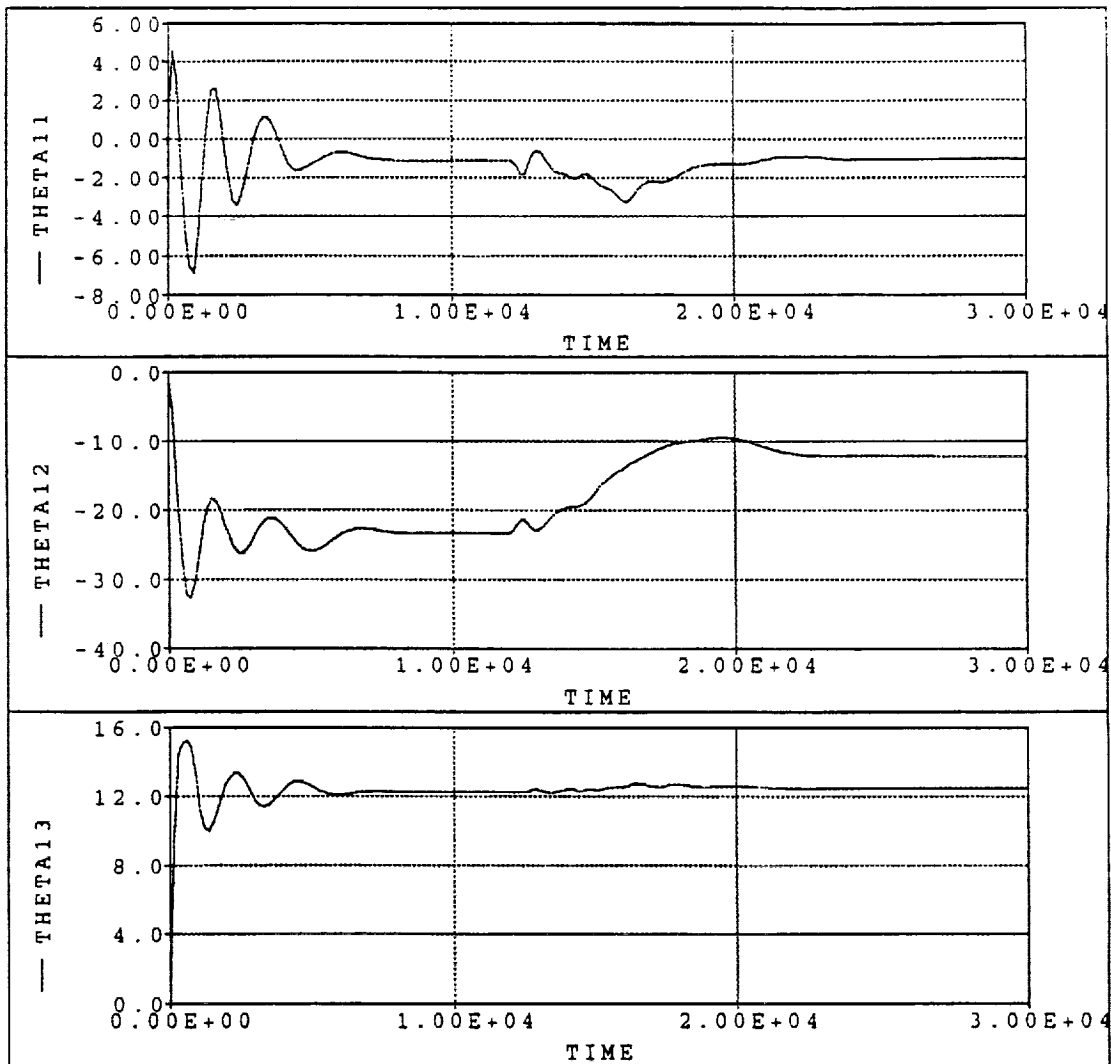


**Figure 3-a: Vehicle Attitude w.r.t. LVLH, SSF CMG, Retraction via SRMS, Aerodynamics (Scenario 1)**

Units:

TIME - seconds

HCMGV - ft-lb-sec

Note: Euler 1-2-3 sequence

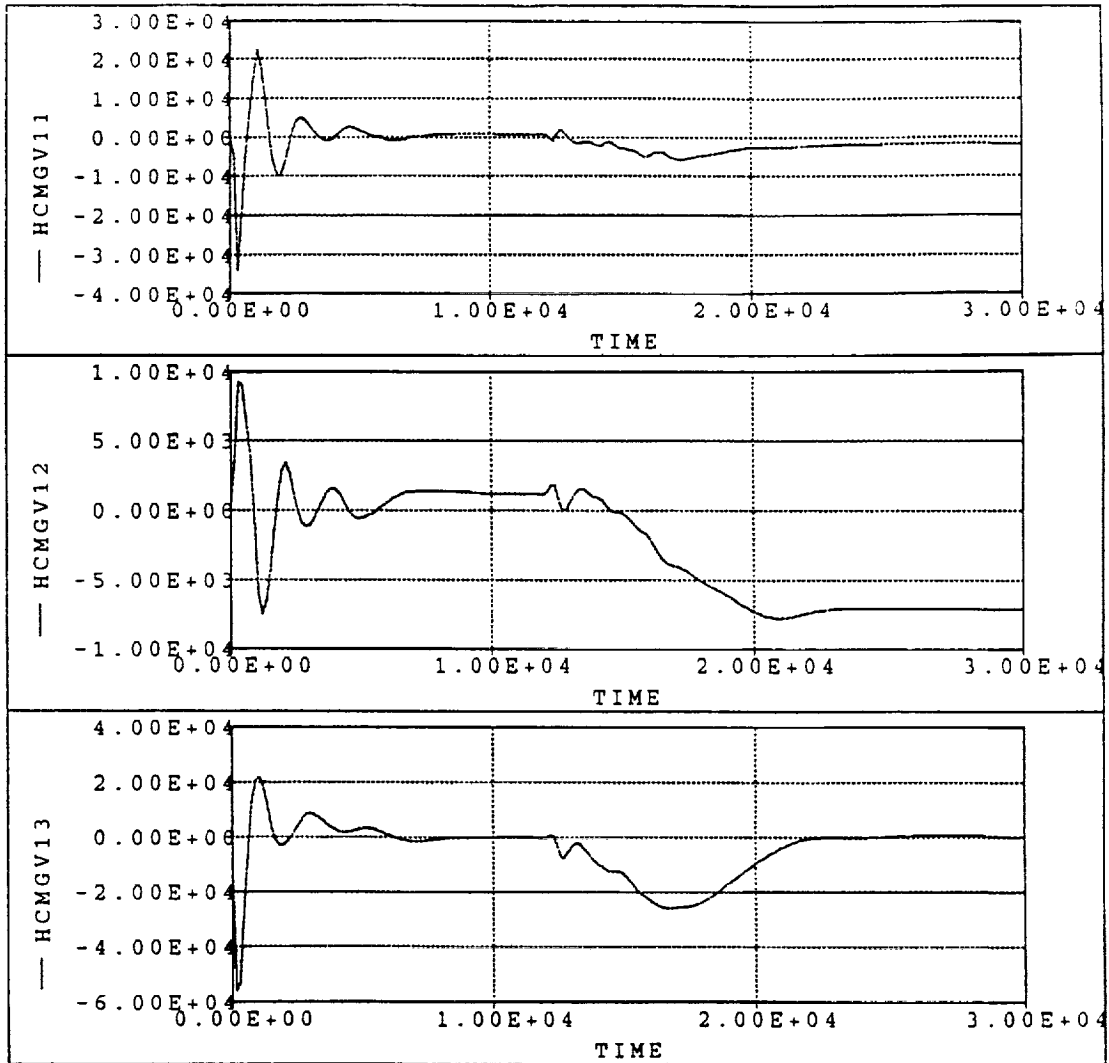


**Figure 3-b: CMG Momentum in SSF Reference Frame, SSF CMG, Retraction via SRMS, Aerodynamics (Scenario 1)**

Units:

TIME - seconds

THETA - degrees

Note: Euler 1-2-3 sequence

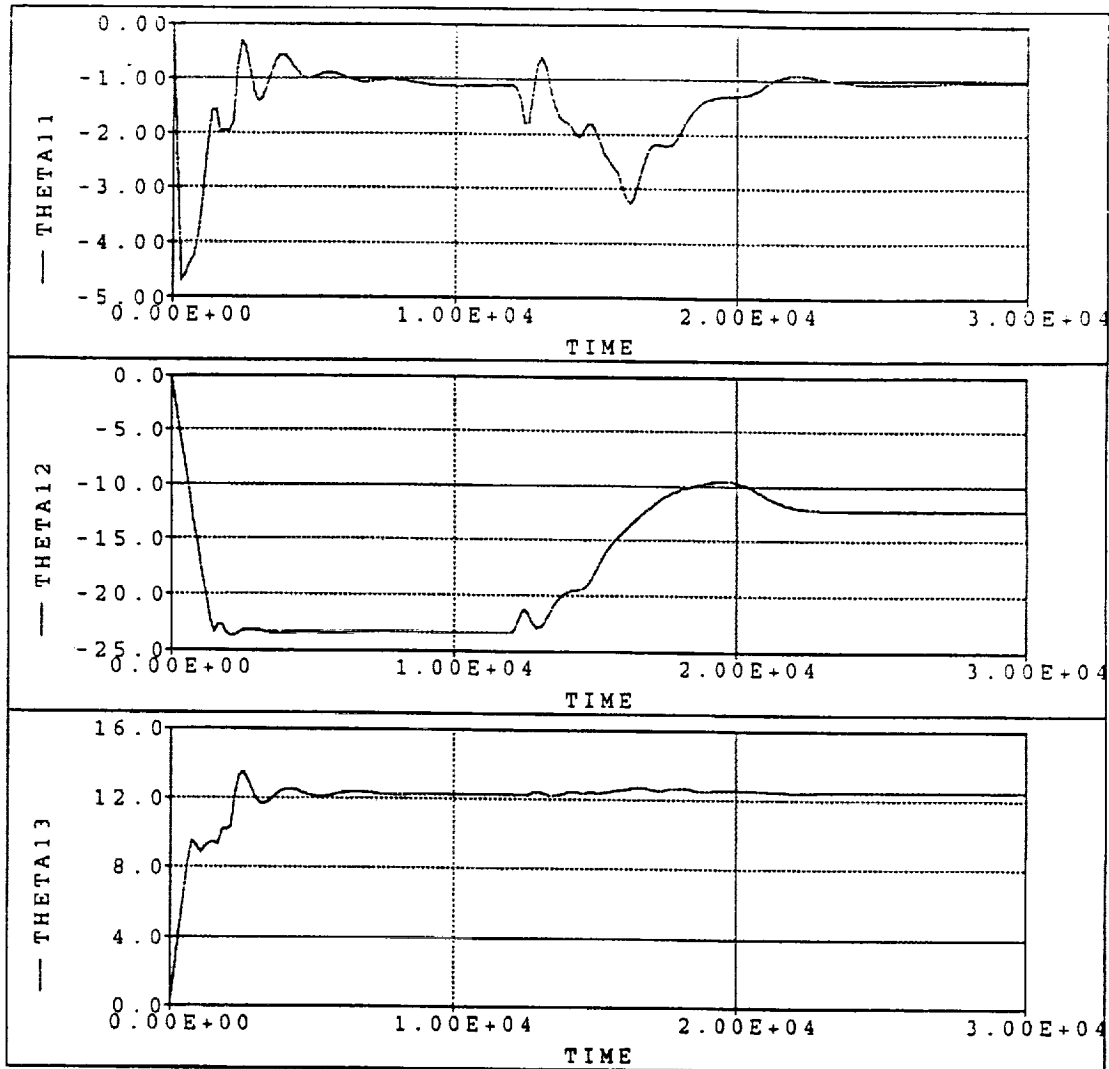


**Figure 4-a: Vehicle Attitude w.r.t. LVLH, SSF RCS/CMG, Retraction via SRMS, Aerodynamics (Scenario 2)**

Units:

TIME - seconds

HCMGV - ft-lb-sec

Note: Euler 1-2-3 sequence

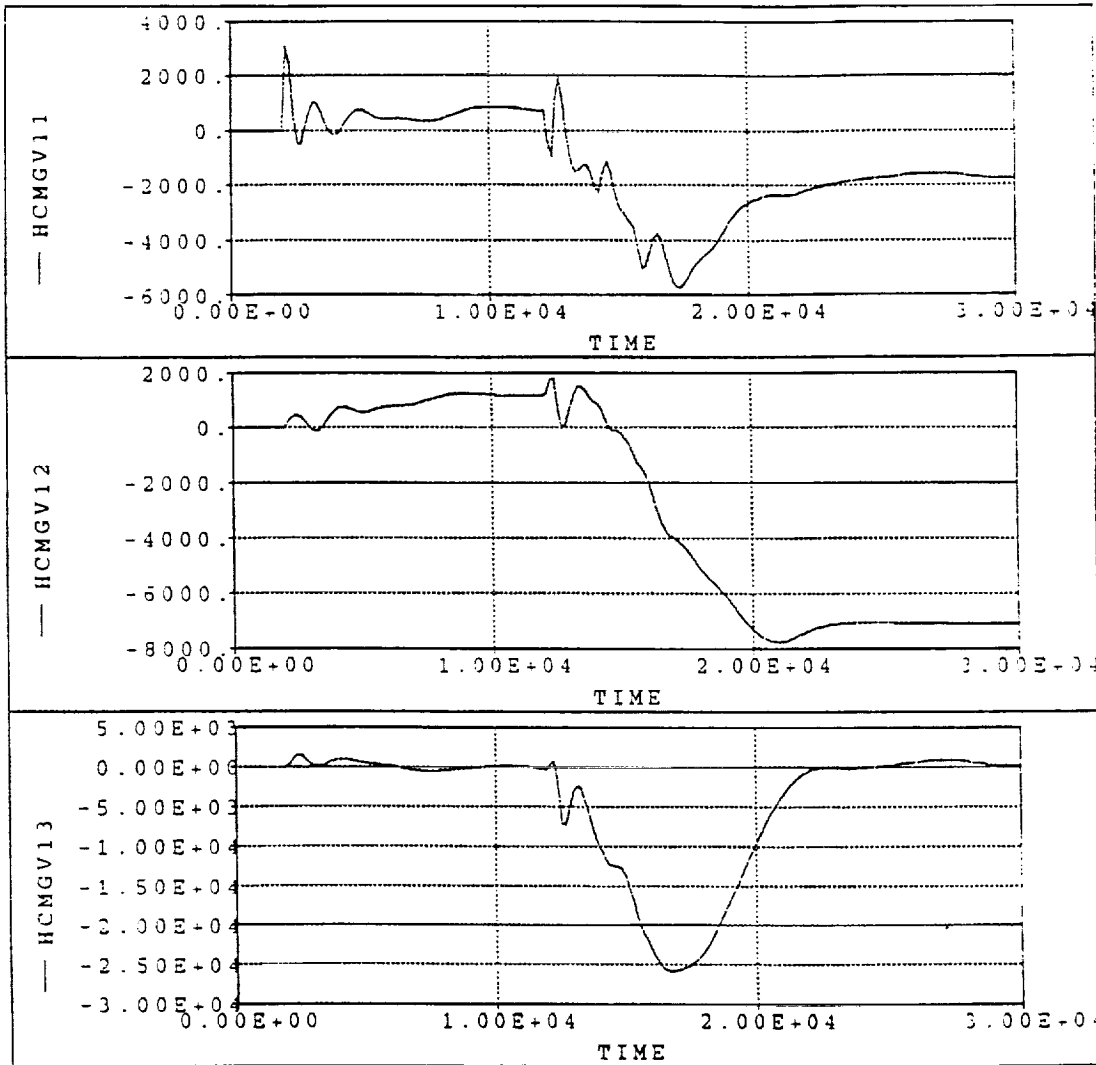


**Figure 4-b: CMG Momentum in SSF Reference Frame, SSF RCS/CMG, Retraction via SRMS, Aerodynamics (Scenario 2)**

Units:

TIME - seconds

THETA - degrees

Note: Euler 1-2-3 sequence

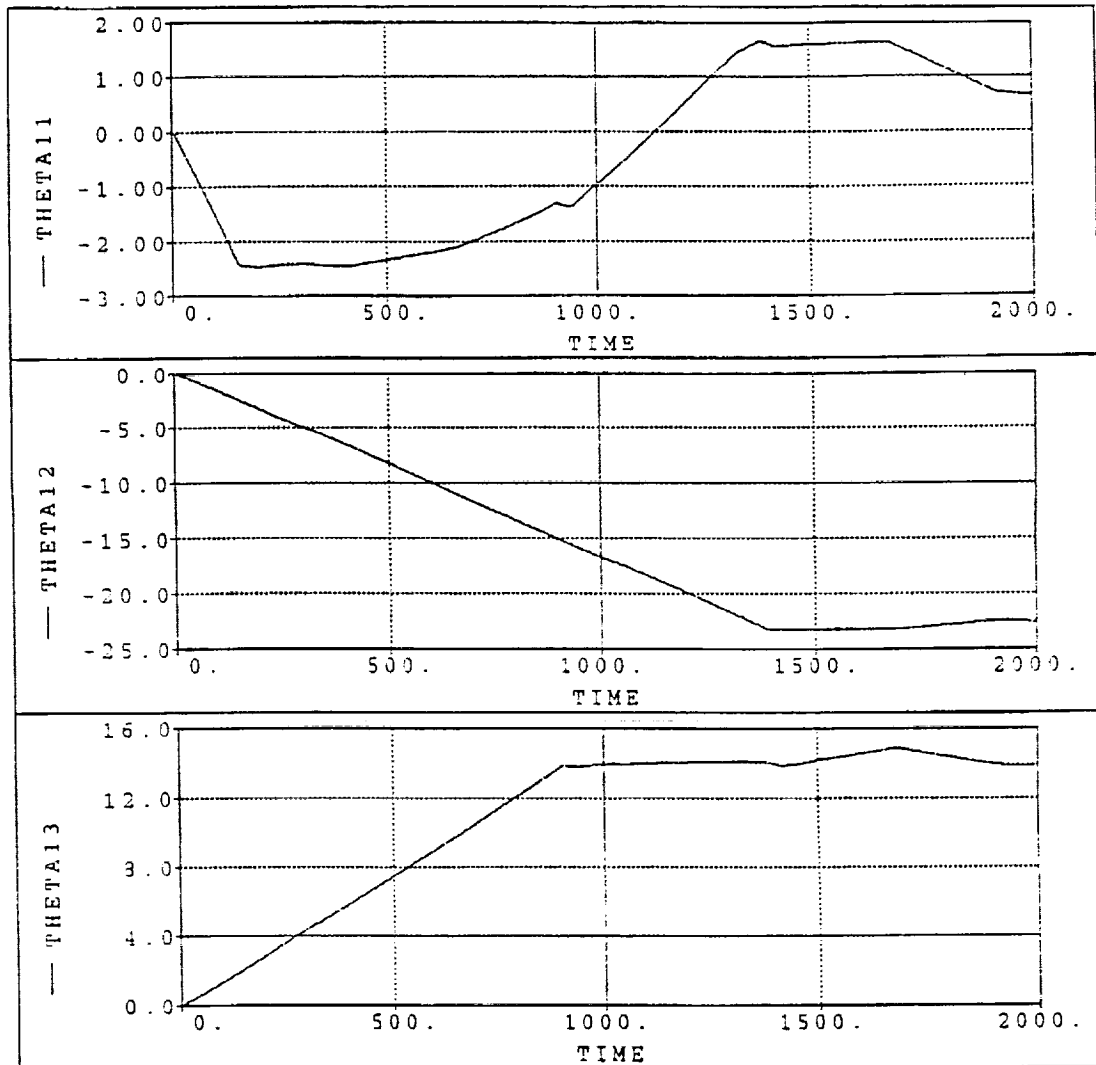


**Figure 5-a: Vehicle Attitude w.r.t. LVLH, SSF RCS, SRMS Brakes on at Capture (Scenario 3)**

Units:  
AE - degrees  
WE - degrees/sec

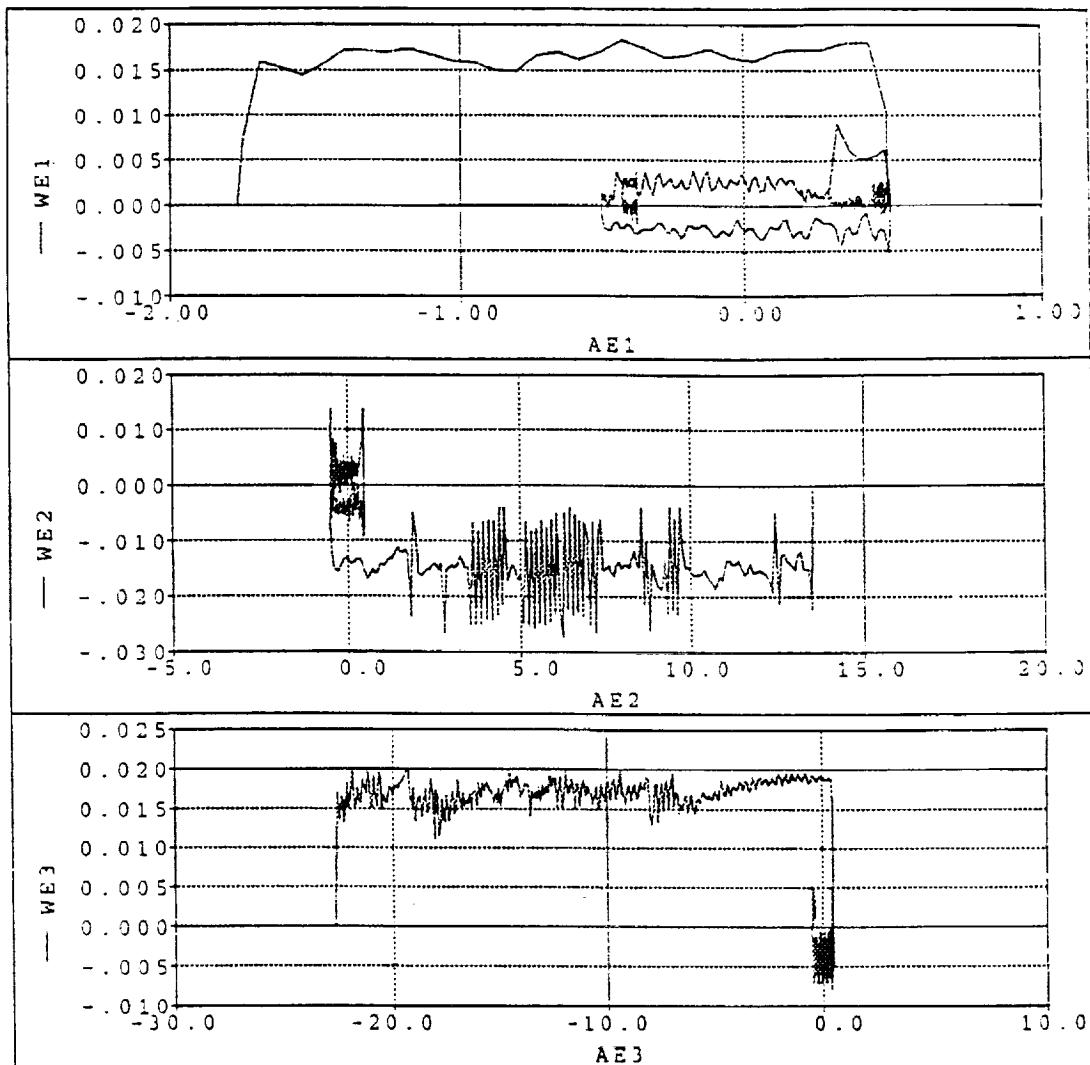


**Figure 5-b: Phase Plane for RCS Maneuver to GG-TEA, SSF RCS, SRMS Brakes on at Capture (Scenario 3)**

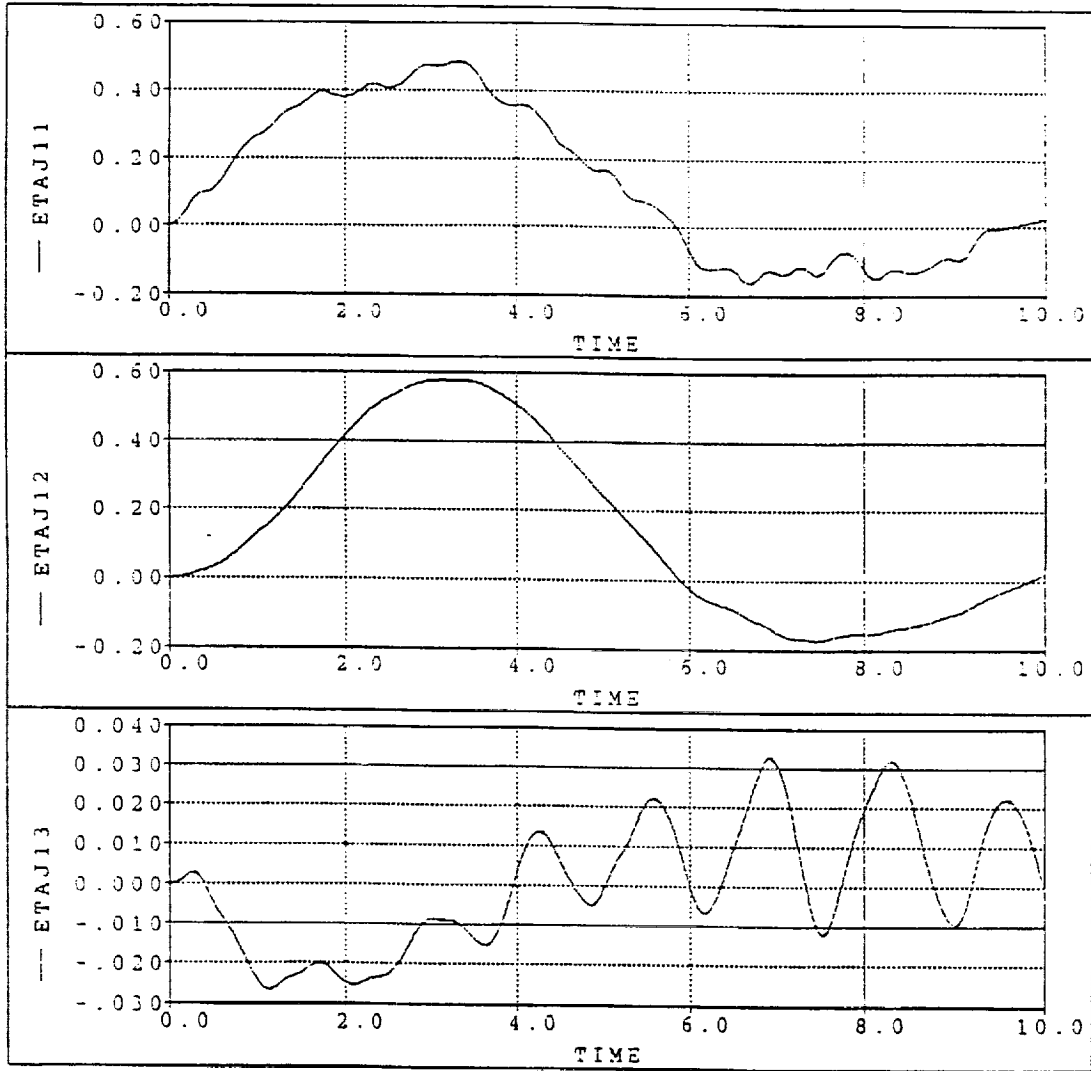


**Figure 5-c: Modal Displacement for RCS Maneuver to GG-TEA, SSF RCS, SRMS Brakes on at Capture (Scenario 3)**



response because the coupling terms between the rigid and deformable body are strong. This figure also shows that the energy in the elastic modes is not zero due to the berthing operation.

## SUMMARY

The previous analysis studied 3 cases using multi-rigid/flexible bodies, a kinematic SRMS model, and the PDR ACS. From these scenarios the following observations were made:

- A CMG only mode may not be sufficient for controlling the combined system of the Orbiter, SRMS, and the SSMB during berthing operations. Results indicate that moving from a gravity gradient attitude to a TEA could result in saturation of the CMG controller.
- An RCS only mode may produce undesirable interaction with the SRMS and needs to be investigated in detail.
- The RCS/CMG mode proves to be the most promising in maintaining control of the combined system of the Orbiter, SRMS, and the SSMB during berthing operations. This control mode also prevents saturation of the CMG/MM system in maneuvering from the gravity gradient attitude to the TEA.
- The use of fixed gains computed at the capture position results in saturation of the CMG/MM control system during berthing operations. This arises from the large variation of the mass properties as the SRMS pulls the SSMB to the Orbiter for berthing.
- The interaction between the rigid and elastic body during the berthing operation needs to be evaluated.
- The CDR control system designed by Honeywell may be able to prevent the problems such as CMG saturation, structure vibration and fuel consumption.

## REFERENCES

1. Space Station Simulation (SSSIM) User's Guide, Dynamic Simulation Revision 1.2, Controller Version C01A, January 15, 1991.
2. System Engineering Simulator On-Orbit Element Simulation Definition Document, LESC-Houston, LEMSCO-24111, January 1991.
3. Singh, R., Schubele, B., and Sunkel, J., "Computationally Efficient Algorithm for the Dynamics of Multi-Link Mechanisms," AIAA Guidance, Navigation and Control Conference, August 14-16, 1989, Boston, Massachusetts.

4. Shabana, A., Dynamics of Multibody Systems, John Wiley & Sons, New York (1989).
5. Space Station Freedom Design Reference Missions (DRM), Revision 1, Working Copy, SSP-TBD, July 1991.
6. "Transmittal of IDEAS Solid Models representing the MTC Phase Review Configuration, based on Level III DPDR data", SSEIC transmittal memo, PSH-312-M091-338, August 2, 1991.

## APPENDIX A

### Instantaneous Inverse Kinematics

The kinematics equations of a robotic manipulator relate the joint displacements to the end-effector position and orientation. For instance, a given set of joint displacements can be used to calculate the resultant end-effector position and orientation. This is referred to as the direct kinematics problem. In this report, the inverse kinematics problem is discussed. For this problem, we find the associated joint displacements when given the desired end-effector position and orientation. Once the joint displacements are calculated, the desired end-effector trajectory can be achieved by moving each joint to the determined value. Since the kinematic equations are nonlinear, numerical methods are used to calculate the desired joint displacements.

To formulate the instantaneous kinematic equations for a general  $n$  degree-of-freedom manipulator arm, we begin with the definition of the vector  $\mathbf{X}_e$ ,  $\mathbf{X}_e \in R^m$ , representing the end-effector motion and  $\mathbf{p}$ ,  $\mathbf{p} \in R^n$ , representing the joint displacements in global coordinates. The degrees of freedom of the manipulator are not necessarily six, but at least six. Letting  $d\mathbf{X}_e = [dx, dy, dz, d\theta_x, d\theta_y, d\theta_z]$  be the  $m \times 1$  vector, which represents the infinitesimal displacements of the end-effector, then the instantaneous kinematic equation for a general  $n$  degree-of-freedom manipulator arm is given by

$$\mathbf{J}\Delta\mathbf{p} = \Delta\mathbf{X}_e \quad (A1)$$

where the dimension of the manipulator Jacobian  $\mathbf{J}$  is  $m \times n$ , and the change in the joint coordinates,  $\Delta\mathbf{p} = [\Delta p_1, \Delta p_2, \dots, \Delta p_n]^T$ , is the  $n \times 1$  vector required to achieve the final position for the end-effector.

The Jacobian represents the infinitesimal relationship between the joint displacements and the end-effector location at the present position and arm configuration. When  $\mathbf{J}$  is of full rank and  $n$  is larger than  $m$ , there are  $(n-m)$  arbitrary variables in the general solution of (A1). The manipulator is said to have  $(n-m)$  redundant degrees of freedom for the given task. Otherwise, there exists at least one direction where the end-effector cannot be moved.

An optimal solution to equation (A1) can be found if we fix the Jacobian at an appropriate arm configuration, and find the optimal solution assuming the Jacobian is of full row rank. We evaluate the solutions to equation (A1) by the quadratic cost function of the joint displacement vector given by

$$G = \frac{1}{2} \Delta \mathbf{p}^T \mathbf{W} \Delta \mathbf{p}, \quad (\text{A2})$$

where  $\mathbf{W}$  is an  $n \times n$  symmetric positive definite weighting matrix. The problem is to find the  $\Delta \mathbf{p}$  that satisfies (A1) for a given  $\Delta \mathbf{X}_e$  and  $\mathbf{J}$  while minimizing the cost function  $G$ . This problem can be solved by using Lagrange multipliers.

Consider the modified performance index

$$g = \frac{1}{2} \Delta \mathbf{p}^T \mathbf{W} \Delta \mathbf{p} + \lambda^T (\mathbf{J} \Delta \mathbf{p} - \Delta \mathbf{X}_e) \quad (\text{A3})$$

where  $\lambda$  is an  $(m \times 1)$  vector of Lagrange multipliers. The necessary conditions that the optimal solution must satisfy are

$$\frac{\partial g}{\partial \mathbf{p}} = \mathbf{W} \Delta \mathbf{p} + \mathbf{J}^T \lambda = 0$$

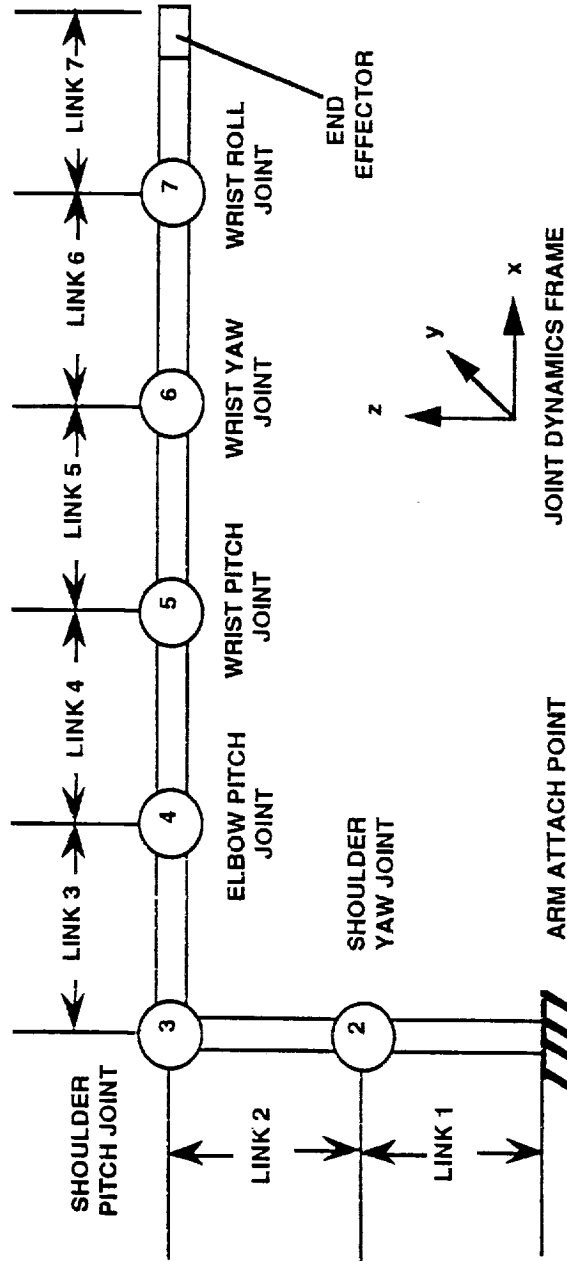
which gives us

$$\Delta \mathbf{p} = -\mathbf{W}^{-1} \mathbf{J}^T \lambda. \quad (\text{A4})$$

Substituting (A4) in (A1) and solving for  $\Delta \mathbf{p}$  by eliminating  $\lambda$ , we have

$$\Delta \mathbf{p} = \mathbf{W}^{-1} \mathbf{J}^T (\mathbf{J} \mathbf{W}^{-1} \mathbf{J}^T)^{-1} \Delta \mathbf{X}_e. \quad (\text{A5})$$

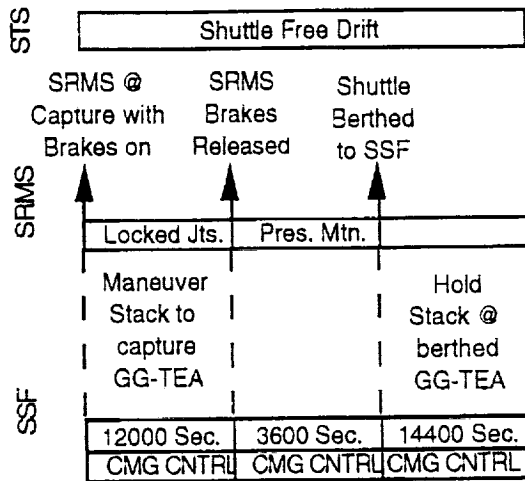
This approach is referred to as a minimum norm solution. Since equation (A5) is nonlinear, iteration of (A5) is often necessary to solve it.



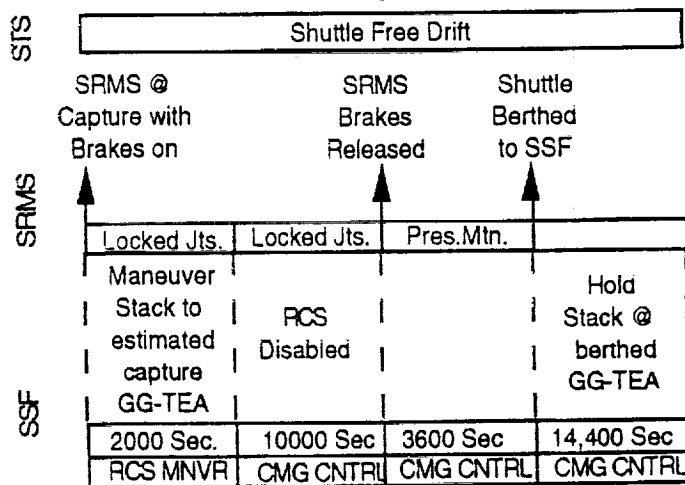
NOTE: Arm in reference configuration (not to scale).

Figure A-1: SRMS Links

## Appendix B



**Figure B-1: Scenario 1**



**Figure B-2: Scenario 2**

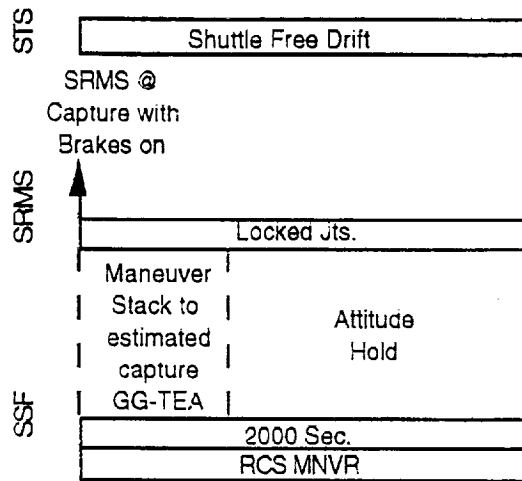
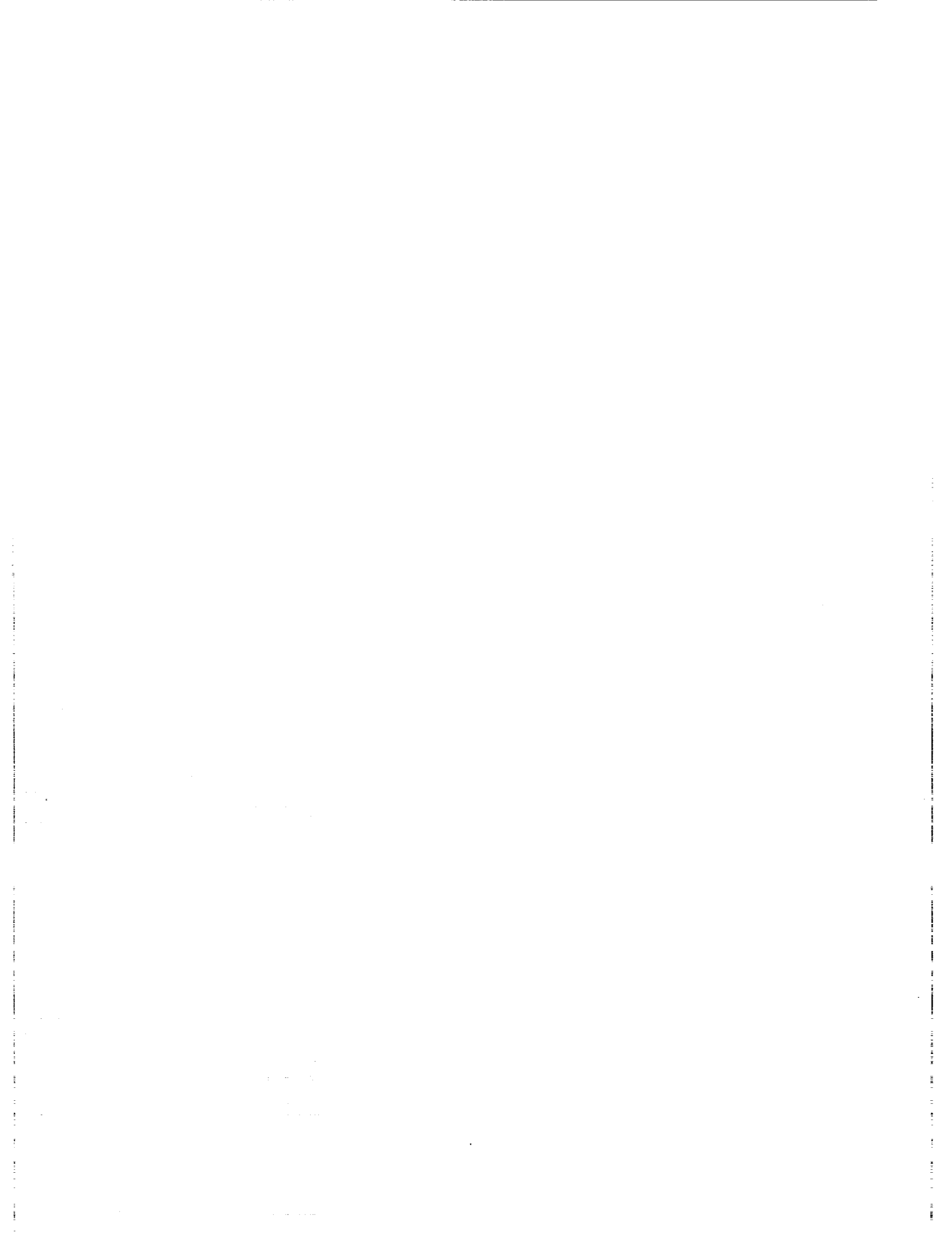


Figure B-3: Scenario 3





# POSTER SESSION

